EFFECT OF SPECIMEN GEOMETRIES ON THE C* Versus da/dt MASTER CURVE OF TYPE 316L STEEL

M.R. Kabiri [1], L. Laiarinandrasana [1], M. Reytier [2]

1) Centre des Matériaux – Ecole des Mines de Paris, BP 87, 91003 Evry Cedex France.

2) CEA Saclay 91191 Gif-sur-Yvette Cedex France.

ABSTRACT

This contribution deals with engineering components working at high temperature and subjected to creep-fatigue loading history. The defect assessment procedures generally use the master curve da/dt versus C* parameter for estimating the creep-crack growth. The ASTM E 1457-98 procedure proposes the rule to establish such a master curve. In particular, it is stipulated that this rule only applies for CT specimens. In SMiRT16, we proposed some practical methodology to produce this master curve on CT specimens :

* by introducing the way to determine the upper and lower limits of relevant experimental points ;

* by adopting the ASTM E 1457-98 method to estimate the creep component of the load line displacement rate ($d\delta/dt_{behavior}$), which is the interesting part of the total displacement rate recorded during the test.

This paper focuses on the application of the procedure proposed in SMiRT16 on specimen geometries other than CT, such are Circumferentially Cracked Round Bar (CCRB) and Double Edged Notched in Tension (DENT) specimens. The master curves issued from all of these specimens are compared. Discussion about the effect of geometry on the master curves will then take place.

Additionally, some finite element analyses have been carried out in order to simulate the creep crack growth using the node release technique. These simulations allow to verify the validity of the proposed expressions of C* and consequently the master curve of the 316L(N) stainless steel.

INTRODUCTION

High temperature structural components are often subjected to non-uniform stress and temperature distribution during service. These conditions may favor localized creep damage in the form of service initiated cracks which can propagate and ultimately cause fracture. A significant portion of the component life can, however, be spent in crack propagation. Therefore, there is considerable interest in developing the technology for predicting creep crack growth behavior.

In SMiRT16 paper [1], we have suggested some recommendations concerning the construction of the da/dt versus C* master curve on CT specimens. In the present paper, we are generalizing this procedure to other specimens (CT, CCRB, and DENT), in order to show the relevance of the master curve of type 316L stainless steel.

At first, we present the characteristics of materials and specimens which this study deals with, then we propose analytical expressions to calculate the load parameter C* for different specimens. 316L(N) master curve plotted respecting the recommendations of the SMiRT 16 especially concerning the domain of validity of this correlation. At last we validate our procedure by a finite element method simulating creep crack growth with node release technique.

EXPERIMENTAL DATA

The creep tests were carried out at the Ecole des Mines de Paris [2] [3]on the “SQ” sheet, Imperial College on the “SD” sheet, and CEA-SACLAY on “VIRGO” sheet of the 316L stainless steel. Tests were performed at constant loads at 550, 575, 600, and 650 °C. The chemical compositions of the materials are given in Table 1.

Table 1 : Chemical compositions of all sheets (weight %)

Sheet	C	Mn	Si	S	P	Ni	Cr	Mo	N	Cu	Co	B
SQ	0.028	1.88	0.3	0.001	0.028	12.46	17.31	2.44	0.077	0.175	0.135	0.0012
SD	0.038	1.83	0.313	0.02	0.036	11.9	17.3	2.46	0.067	0.27	--	--
VIRGO	0.022	1.8	0.38	0.02	0.021	13.3	17	2.25	0.032	0.032	--	0.0014

The conventional tensile properties of all sheets in different temperatures are given in Table 2.

Table 2 : Tensile properties of all sheets of 316L stainless steel

Sheet	Temperature (°C)	Elastic Modulus (MPa)	Yield strength (MPa)	Tensile strength (MPa)
SQ	575	144000	149	428
	600	144000	146	407
	650	144000	141	367
SD	650	148000	167	403
VIRGO	550	144000	112	361

In order to verify the specimen effect on da/dt versus C* master curve, three specimens geometries were analyzed : compact tension (CT), circumferentially cracked round bar (CCRB), and double edge notch tension (DENT). These specimens were fatigue pre-cracked at room temperature. They were instrumented to measure both the load line displacement δ(t), and the crack length a(t). More details on the specimens geometries are reported in Figure 1.

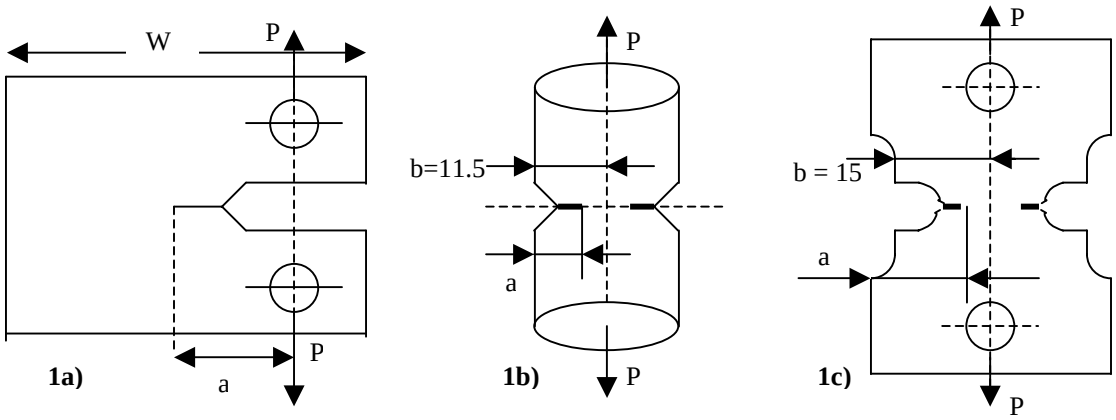

Figure 1 : Specimens geometries a) CT; b) CCRB; c) DENT. All dimensions are given in mm.

where :

- P is the applied load (N), a is the crack depth (mm), and W is the width of the CT specimen.
- B is the thickness of CT, and DENT specimens. For DENT specimens, B = 10mm
- b is the half width of DENT specimen , and the radius of CCRB specimen.

The characteristic dimensions of EMP's CT specimen (4CT) are : W = 40mm, B=10mm, those of Imperial College (3CT) are W = 50, B=23.8mm and W = 25mm, B=12.7mm, and those of CEA (2CT) are side-grooved, W=50mm, B_{total} =25mm, B_{net} = 20mm. In the following, CT specimens will be analyzed under plane strain conditions. Experimental data for all specimens consist of files containing the time, the load-line displacement and the crack depth. For EMP's CT and CCRB specimens, data are available in [2]. It should be remembered that CCRB specimens are interesting in the sense that they need neither plane strain nor plane stress conditions to model them. In the authors knowledge, there are no available experimental data for other specimen types, apart from 2 DENT issued from [3]. Unfortunately, they are not complete as it can be seen in figure 2. Nonetheless, those tests will be utilized in the following and analyzed under plane stress conditions [3].

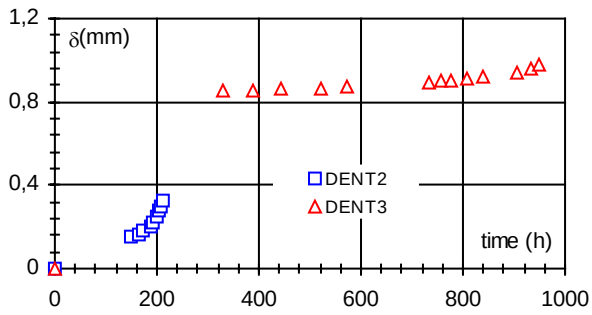

Figure 2 : Creep tests of DENT specimens.

CREEP BEHAVIOR

For the time-dependent behavior of all specimens submitted to a constant load, both primary and secondary creep were taken into account, with standard creep laws. These laws as well as the tensile stress-strain one are given in the following :

Plasticity : $\varepsilon = B_0 \sigma^n$ (1) , Primary creep : $\varepsilon = B_1 \sigma^{n_1} t^{p_1}$ (2) , Secondary creep : $\dot{\varepsilon} = B_2 \sigma^{n_2}$ (3), where :

- ε is the strain (mm/mm) and $\dot{\varepsilon}$ is the strain rate (mm/mm.h)
- σ is the applied stress (MPa)
- t is time (h)
- B_0, B_1, B_2, n, n_1, n_2, and p_1 are some constants.

The values of different constants of plasticity and creep laws are given, for each sheet in Table 3.

Table 3 : Values of plasticity and creep laws constants

Sheet	Temperature (°C)	B_0	n	B_1	n_1	p_1	B_2	n_2
SQ	575	--	--	9E-14	4	0.43	--	--
	600	2.86E-8	2.4968	1.441E-14	4.642	0.5135	1.6325E-25	7.69
	650	--	--	2.633E-14	4.7463	0.57	6.95E-25	7.69
SD	650	3.838E-25	2.872	5.863E-13	4.233	0.565	1.018E-25	9.407
VIRGO	550	--	--	4.414E-12	3.361	0.411	6.71E-24	8.4

DETERMINATION OF C*

The load parameter C* is calculated from the load-line displacement rate $d\delta_{exp}/dt = \dot{\delta}_{exp}$ which, according to [1], is a sum of a part due to the creep behavior noted $\dot{\delta}_C$ and a part due to the structure response related to the crack growth noted $\dot{\delta}_S$:

$$\dot{\delta}_{exp} = \dot{\delta}_C + \dot{\delta}_S \quad (4)$$

For each specimen type, we calculate C* parameter using only the part of the load-line displacement rate due to the creep behavior. We assume that the structural term $\dot{\delta}_S$ is uniquely due to the crack advance (elastic-plastic term, not time dependent) and may be estimated, for instance in the EPRI [4], the R6 rule [5] and the French A16 guide [6] because this load-line displacement is directly related to J-integral . It's then easy to deduce this term as follows :

$$\text{For CT and DENT specimens : } \dot{\delta}_C = \dot{\delta}_{exp} - \frac{\dot{a} B}{P}\left[\frac{2K_I^2}{E^*} + (n+1)J_P^{EPRI}\right] \quad (5)$$

where :

- $\dot{a} = da/dt$ is the crack growth rate (mm/h)
- K_I is the stress intensity factor (MPa.mm$^{1/2}$)
- $E^* = E/(1-\nu^2)$ in plain strain and $E^* = E$ in plane stress, where E is the Young's modulus.
- n is the stress exponent according to (1).
- J_P is the fully plastic component of the J-integral calculated using EPRI method [4].

$$\text{For CCRB specimen : } \dot{\delta}_C = \dot{\delta}_{exp} - \frac{2\pi \dot{a} R}{P}\left[\frac{2K_I^2}{E} + (n+1)J_P^{EMP}\right] \quad (6)$$

where :

- R is the uncracked ligament of CCRB specimen type, where R = (b – a)
- $J_P^{EMP} = \frac{n-1}{n+1}\frac{P\delta}{2\pi R^2}$ according to [2], with δ the plastic load line displacement

It should be mentioned that the EPRI method does not provide J_P formulation for CCRB specimens. Thus, we can formulate the load parameter C* for each specimen type as following :

For the CT specimens, $$C^*(CT) = \left[2 + 0.522\left(1 - \frac{a}{W}\right)\right]\frac{n_2}{n_2+1}\frac{P\dot{\delta}_C}{B(W-a)} \quad (7)$$

For the CCRB specimens : $C^* = \frac{n_2-1}{n_2+1}\frac{P\dot{\delta}_C}{2\pi R^2}$ (8) and for the DENT specimens : $C^* = \frac{1}{2}\frac{n_2-1}{n_2+1}\frac{P\dot{\delta}_C}{B(b-a)}$ (9)

DOMAIN OF VALIDITY OF THE da/dt versus C* CORRELATION

According to [1], we assume that the lower limit of the $\dot{a}$ versus C* curve is corresponding to the starting point of the last transient stage of creep. For 316L(N) stainless steel, this point corresponds to the C* minimum value. The upper limit should discriminate the tertiary creep stage. To do this, we use the reference length concept [1][2], the secondary creep regime is established as long as $\dot{\delta}_C$ is proportional to $(W-a)B_2\sigma_{ref}^{n_2}$, where σ_{ref} is the reference stress of specimens given according to [4] and [2]. In the following, only experimental points corresponding to these descriptions will be selected.

THE MASTER CURVE OF 316L(N)

da/dt Versus C* correlation of "SQ" sheet

Let us focus on creep tests performed at the Ecole des Mines de Paris : 4 CT, 14 CCRB and 2 DENT. We first, plot the da/dt versus C* curve for each specimen type. Results (Figure 3) show that there is a unique correlation for each specimen.

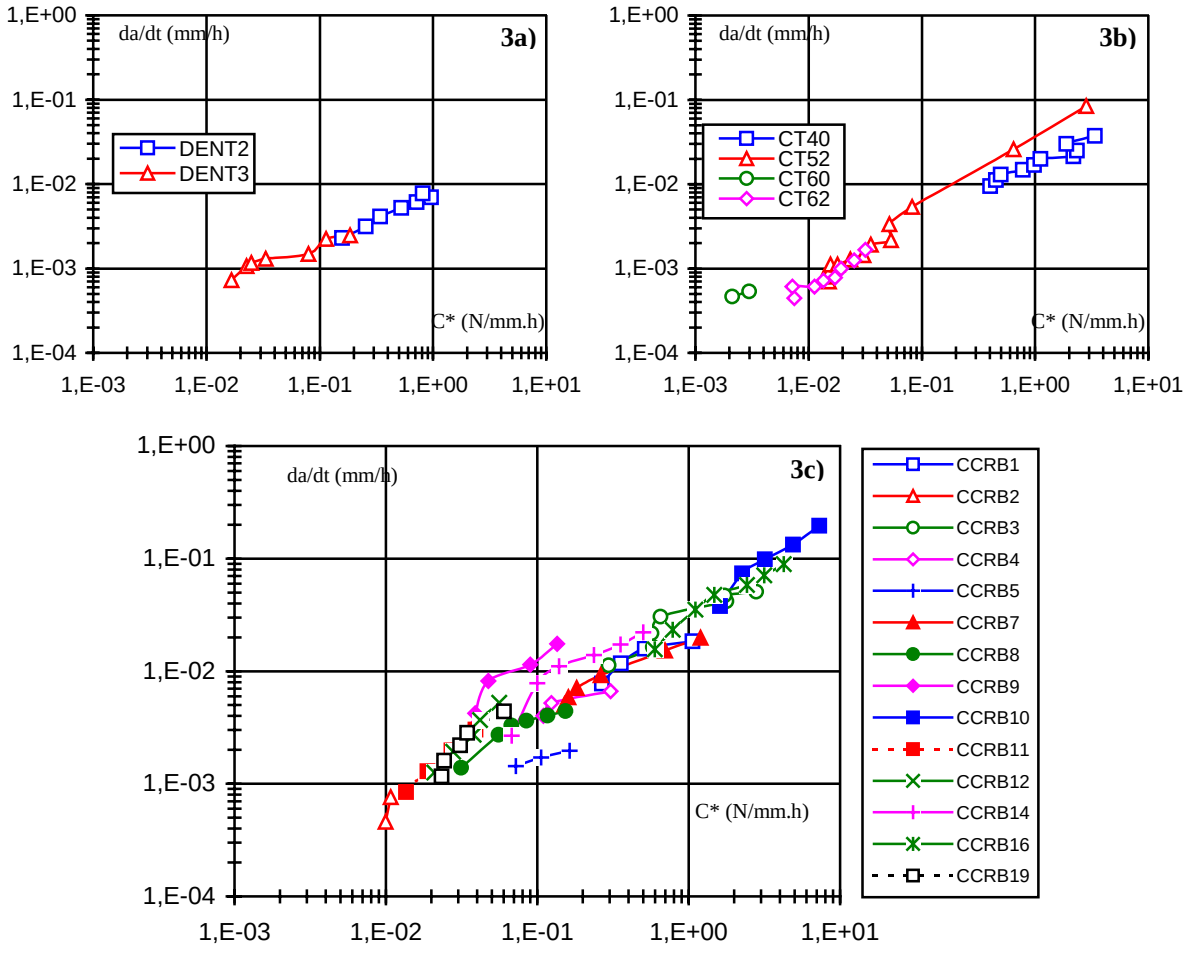

Figure 3 : da/dt versus C* curve for each specimens type : 3a) DENT, 3b) CT and 3c) CCRB

Let us now merge the results illustrated in figure 3 into a unique da/dt versus C* curve. All of the experimental points of the three specimens are utilized in order to fit a power law $da/dt = AC^{*q}$.

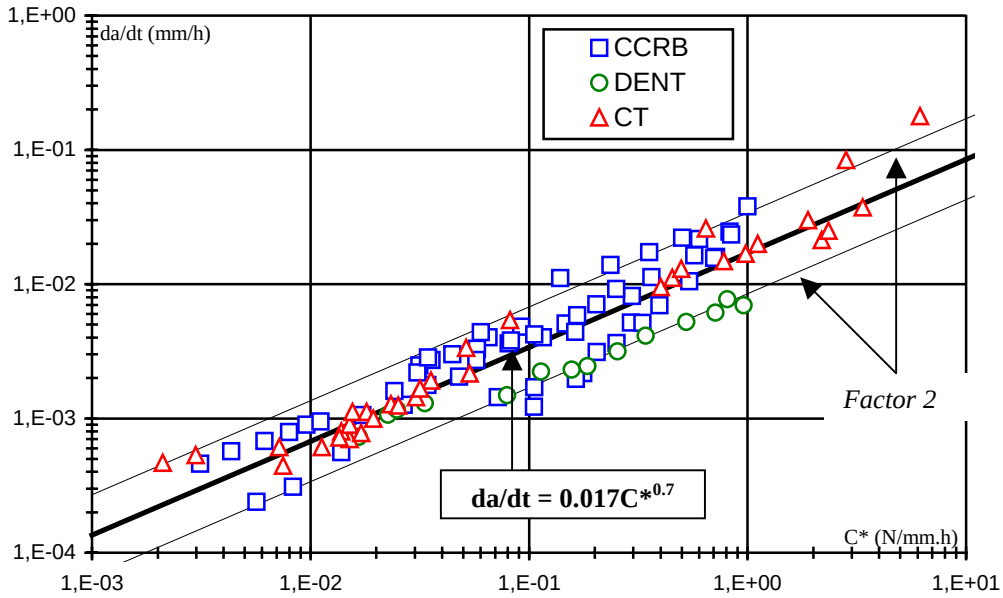

Figure 4 : da/dt versus C* curve for "SQ" sheet of 316L(N) – All specimens.

Fig.4 shows that, within a scatter band of about factor 2, a unique correlation is obtained for 3 specimen geometries and 3 temperature tests ranging from 550°C to 650°C. By fitting coefficients A and q of the $da/dt= AC^{*q}$ it comes out that A = 0.017 and q = 0.7 which are very close to the values given earlier [1] on CT specimen type (A=0.016, q =0.71). So, for the "SQ" sheet, we can conclude that there is no effect of specimen geometries on the da/dt versus C* curve.

da/dt Versus C* correlation of "SD" and "VIRGO" sheets

Figure 5a) displays the results for the "SD" sheet of the 316L(N) tests. We note a correlation da/dt versus C* load parameter. In figure 5b), a unique correlation da/dt versus C* characterizes the creep crack growth in the "VIRGO" sheet.

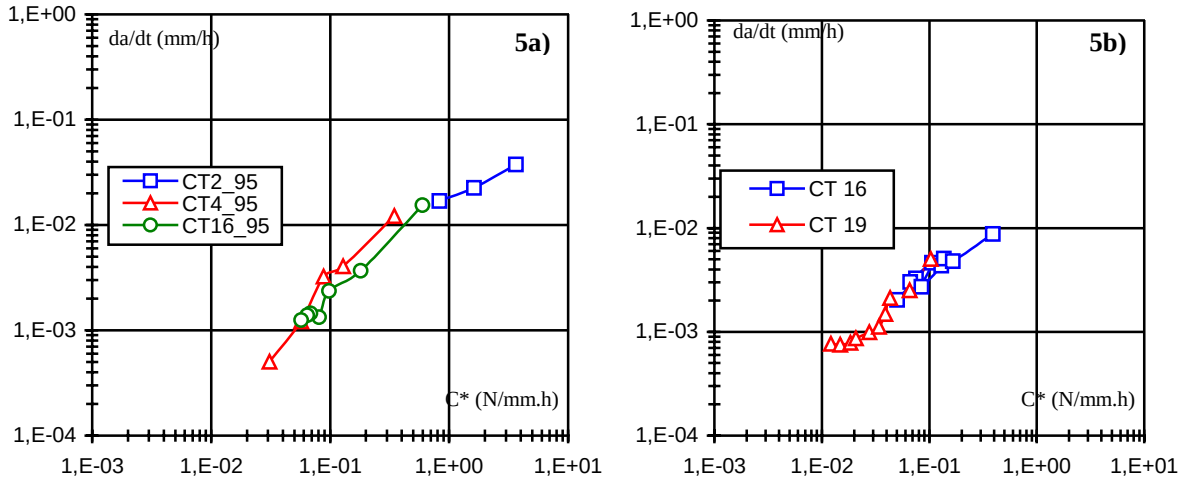

Figure 5 : da/dt versus C* curve for CT specimens type : a) "SD" sheet, b) "VIRGO" sheet.

Master curve of the 316L(N) stainless steel

Now we plot in the same diagram (figure 6) the da/dt versus C* of all specimens types of the three sheets of 316L(N) stainless steel.

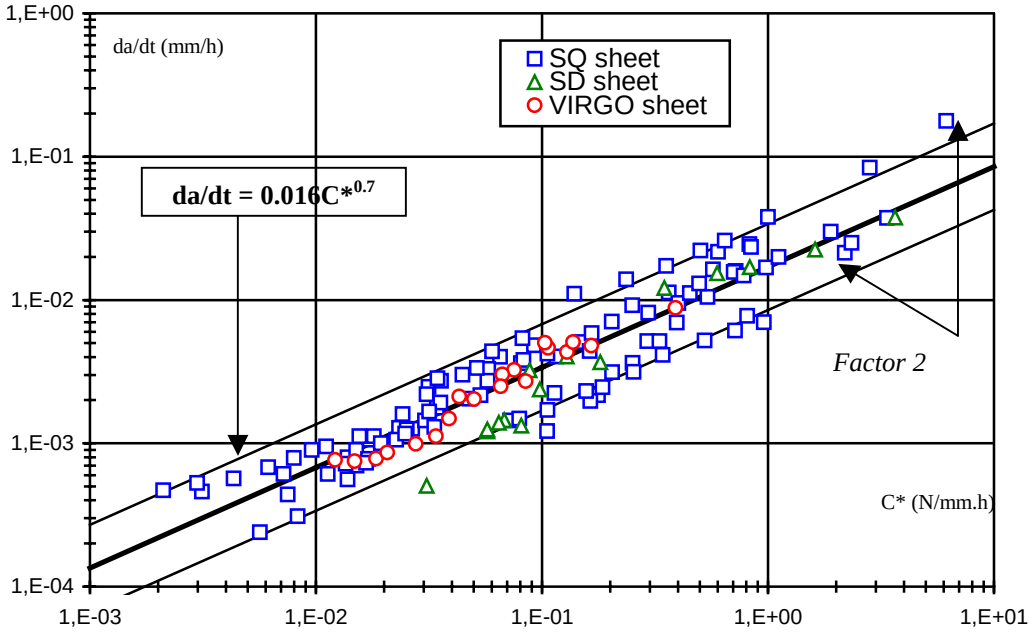

Figure 6 : da/dt versus C* master curve of the 316L(N) stainless steel.

Fig.6 shows the results for the 316L(N) stainless steel tests. Experimental points corresponding to three sheets are represented is the same figure. The fitted coefficients (A = 0.016, q = 0.7) are the same as those established on the "SQ" sheet. The same result was found by Piques [2] using the reference length concept [1].

FINITE ELEMENT SIMULATIONS

The purpose of this part is to validate the aforementioned results by simulating creep crack growth tests. The technique used in these computations is based on node release [8]. The main principle of this technique consists in releasing adjacent nodes with respect to the experimental a(t). The mesh size grain is about 50µm. After each node releasing an equilibrium state is checked. This leads to redistribution of the initial load of the released nodes over the surrounding nodes. The creep behavior was determined at 600°C using the DID model (Double Inelastic Deformation) [9] [10]. Typically only primary and secondary creep regimes were taken in account. Simulated tests were 2CT, 8CCRB, and 2 DENT specimens. The values of C* contour integral are computed all along the F.E. analysis.

We explain below, a worked example of the CCRB1 specimen tested at 600°C, with initial crack ratio of a/b = 0.45 and applied load of 52630N. According to the SMiRT 16 [1] recommendations, we simulate this test from the beginning, including an incubation time about 25h (if $t \leq 25h$, $\Delta a = 0$), to the time corresponding to the upper limit of domain of investigation. During 180h of creep test the crack advance is $\Delta a = 550\mu m$

12 nodes have been selected to be progressively released (fig. 7a), and 12 contours have been defined surrounding each position of the crack tip in order to calculate the C* contour integral . We studied the sensitivity of the contours upon the C* values. Our results show that the load parameter C* has the same value independently of the contours. In figure (7b), we show the Von Mises equivalent stress contour map with the deformed meshes after 180h of creep simulation.

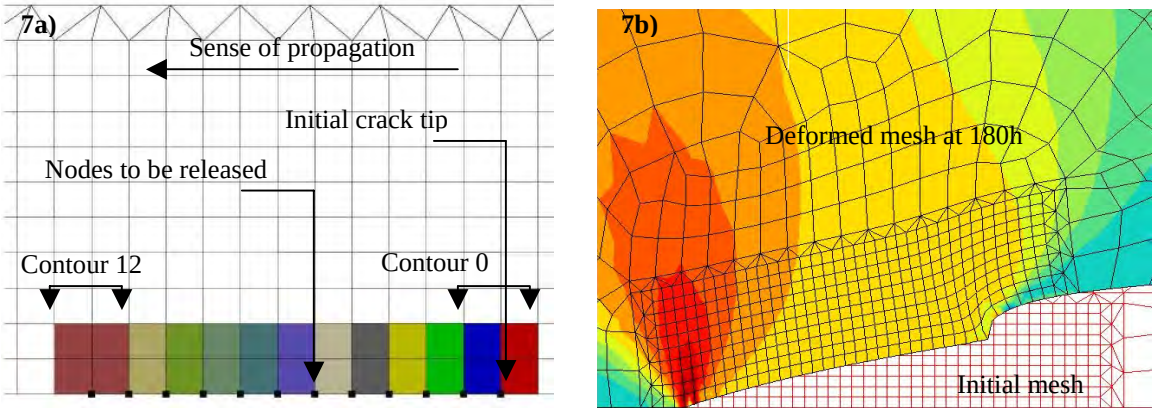

Figure 7 : Mesh of CCRB1 specimen : a) Nodes and contours positions b) Results after releasing.

In figure 8, comparisons are made between selected "experimental" curves issued from figure 6 and their computed counterparts. Note that da/dt scale has been changed (range = 10^{-4} to 10^{-2}) for a good comparison. In the following comments, full symbols deal with simulated value whereas empty ones will refer to experiments. In figure 8a) the CCRB1 curves (square symbols) indicate an excellent argument between experimental and numerical simulations. For CCRB11 (triangle symbols) and CCRB14 (diamond symbols), the shift between experimental/simulated curves is uniquely due to $\dot{\delta}_C$ difference. This can be proved from equation 8.

Figure 8b) shows again the accordance between numerical simulation and experimental curve for CT52 (square symbols) and DENT3 (triangle symbols). For this latter, although the experimental data is incomplete, a portion of stationary creep stage seems to appear (see figure 2). The good agreement between simulation and experiment for DENT3 means that the experimental $\dot{\delta}_C$ is well fitted by the strain rate obtained from the constitutive equation (DID model). That is not the case for DENT2 specimen. In figure 2, only the end of the experimental curve is available. In order to calculate a correct C* value, an interpolation of $\dot{\delta}_C$ is needed. However, it should be noted that the experimental values are in the same trend as for other specimens.

Finally, the node release technique used to simulate creep crack growth provides excellent results. Hence, figure 6 can be reproduced with finite element simulated curves allowing to get the same conclusions. Furthermore finite element C* values for creep propagating cracks confirm analytical formulations as in equations (7) (8) and (9).

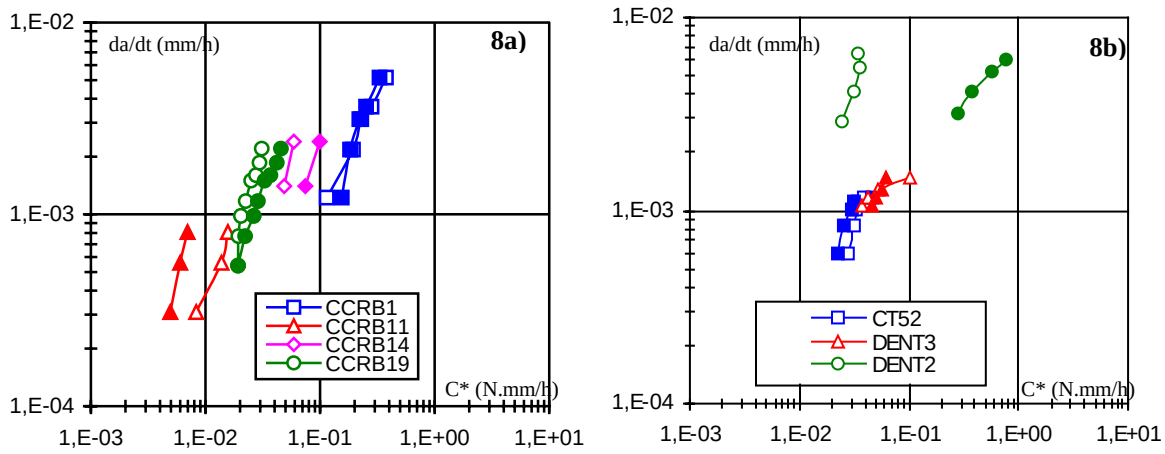

Figure 8 : Comparison between experiment and simulation. 8a) CCRB ; 8b) CT and DENT

CONCLUSION

The ASTM E 1459-98 standard [11] covers the determination of creep crack growth on CT specimens at high temperature on a creep ductile materials when the use of C* load parameter is relevant. This procedure can be extended to other specimens . In the case of 316L(N) stainless steel, three specimens (CT, CCRB, and DENT) were tested at various temperatures (550, 575, 600, and 650°C).

In order to characterize the creep crack growth of this material, we extract the part due to crack growth from the load line displacement rate. We propose some expressions to calculate C* for CCRB and DENT specimens, and we limit the domain of investigation using the reference length concept.

Creep crack growth on 27 specimens of three sheets (SQ, SD and VIRGO) were analyzed. For each test the new procedure [1] was respected. Finite element simulations on 12 specimens were carried out at 600*C using the node release technique. These investigations show that, over a large temperature range [550, 650°C], for a crack ratios such $0.42 < a/b < 0.69$, and for different specimens types : CCRB, CT and DENT, no effect of geometry has been observed. Finally , a unique master curve da/dt versus C* can describe the creep crack growth of 316L(N) stainless steel. The fitted coefficients according to $da/dt = AC^{*q}$ are ($A = 0.016$, $q = 0.7$).

REFERENCES

[1] Laiarinandrasana, L., Piques, R., Kabiri, M.R., Drubay, B., Master curve da/dt vs C* for creep and creep-fatigue crack growth on CT specimens. Proc. Of the 16th International Conference on Structural Mechanics in Reactor Technology, Washington, U.S.A., August 2001.

[2] Piques, R., Mechanics and mechanisms to crack initiation and growth under viscoplastic conditions in an austenitic stainless steel. Thesis (in French), Ecole Nationale Supérieure des Mines de Paris (1989).

[3] Maas, E., Creep crack growth in the austenitic stainless steel Z3-CND17-13. Thesis (in French), Ecole Nationale Supérieure des Mines de Paris (1989).

[4] Kumar, V., German, M.D. and Shih, F., An engineering approach for elastic plastic fracture analysis. NP-1931, Project 1237-1, Topical report, EPRI (1981).

[5] Milne, I., Ainsworth, R.A., Dowling, A.R., Stewart, A.T., Assessment of the Integrity of Structures containing Defects. CEGB Report R/H/R6 – Revision 3 (1986)

[6] Drubay, B. et al, A French guideline for defect assessment at elevated temperature and leak before break analysis. Proc. Of 9th International Conference on Nuclear Engineering, paper 713, Nice France April 2001

[7] Curtit, F., Creep-fatigue propagation of semi-elliptical crack at 650°C in 316L(N) stainless steel plates with or without welded joints . Thesis (in French), Ecole Nationale Supérieure des Mines de Paris (1999).

[8] Besson, J., Foerch, R., Large scale object-oriented finite element code design. Computer Methods in Applied Mechanics and Engineering 142, pp 165-187, (1997).

[9] Cailletaud, G., Saï, E., Study of plastic/viscoplastic models with various inelastic mechanisms. International Journal of Plasticity 11 (8), pp 991-265, (1995).

[10] Laiarinandrasana, L., Piques, R., Creep-fatigue crack initiation in 316L stainless steel : Comparison between stress and strain calculation methods. International HIDA Conference, Commissariat à l'Energie Atomique (CEA)/INSTN, Saclay/Paris, France, April 1998.

[11] ASTM E 1457 – 98, Standard Test Method for Measurement of Creep Crack Growth Rates in Metals (1998)